Electropolymerization of Pyrrole-Based Ionic Liquids on Selected W	/ireless
Bipolar Electrodes	

Han	Chen.	Jared 1	L. And	erson.* I	Robby	ηK.	Anand*

Department of Chemistry, Iowa State University, Ames, Iowa 50011, United States

**Keywords:** electropolymerization, conductive polymeric ionic liquid, bipolar electrochemistry, microfluidics, dielectrophoresis

E-mail: andersoj@iastate.edu, rkanand@iastate.edu

Submitted: December 30, 2021

<sup>\*</sup> To whom correspondence should be addressed

#### Abstract

This paper describes an electropolymerization-based on-chip valving system, accomplished by electrosynthesis of conductive polymeric ionic liquid (CPIL) films at selected points within an array of bipolar electrodes (BPEs), in which each of these wireless electrodes spans an IL-aqueous phase boundary. The low viscosity and high hydrophobicity of the CPIL precursor allows it to be patterned by established microfluidic methods. This advancement has the potential to impact microscale analysis because it allows on-demand creation of solid CPIL microstructures at locations specified by microfluidics, phase boundaries, and electrode potential. To achieve this outcome, an imidazolium-based IL was functionalized with a pyrrole moiety, and the viscosity was tuned by choosing the appropriate counter-ion to form a CPIL with the desired viscosity, hydrophobicity, and oxidation potential. This monomer species was then introduced into a microfluidic device, which was pre-filled with an aqueous buffer solution. The device comprised many parallel microchannels lined with nanoliter-scale chambers. BPEs interconnected the channels such that the BPE tips were each aligned to a chamber opening. The electrodes contacting the outermost channels were connected directly to a power supply and functioned as driving electrodes. The CPIL displaced the buffer in the channels and established a phase boundary at the opening of each chamber, thereby digitizing the aqueous phase. Finally, an alternating square waveform (under mode 1) was applied for 5 min to yield immobilized polymer films at a location defined by the BPE poles. In total, three modes have been developed and three corresponding polymer film patterns were formed. Under mode 2, a DC power supply was used to achieve a dissymmetrical polymer film pattern, and under mode 3, a regional polymer film pattern was formed under an AC potential with a DC offset. Our preliminary results demonstrate that the generated polymer films are immobile and sufficiently thick to seal the chambers at room temperature over the duration of our observation window (50 min), and this seal is maintained even at elevated temperatures that induce partial evaporation of the chamber contents. A key point is that this method is compatible with a preceding step – dielectrophoretic capture of single melanoma cells within the nanoliter-scale chambers.

#### Introduction

An unexpected response from a minority of cells can have a dramatic impact on the development, prognosis, and treatment of disease. <sup>1,2</sup> For example, in the progression of cancer, a resistant minority of circulating tumor cells (CTCs) leads to the development of refractory metastases at relapse. <sup>3, 4</sup> However, the enormous value of CTCs has not been completely realized because the detection and isolation of CTCs is incredibly challenging due to their extreme rarity and varied physical and biological characteristics. <sup>5</sup> Previously, a unified platform for marker-free selection of CTCs has been developed. This platform accomplishes single-cell sequestration of CTCs into an array of reaction chambers by dielectrophoresis (DEP) at wireless bipolar electrodes (BPEs), thus creating conditions appropriate for integrated selection, fluidic isolation, and electrical lysis of single cells in parallel. <sup>6</sup> During the fluidic isolation step, a hydrophobic ionic liquid (IL), was employed as an immiscible phase to seal the reaction chambers and function as a conductor to facilitate electrical lysis of CTCs. This immiscible phase material is fluid and prone to intrusion within the chambers if pressure imbalances develop in the device. Therefore, to better facilitate on-chip single-cell capture and analysis, a more stable phase boundary is needed, and the potential candidate material should be rapidly solidified under mild conditions. To achieve this requirement, we 1) synthesized a conductive polymeric ionic liquid (CPIL) that can simultaneously function as electropolymerizable unit and supporting electrolyte, 2) developed an on-demand valving system, which accomplished by electropolymerization of CPIL films at selected points within an array of BPEs in the presence of an adjacent aqueous phase, and 3) evaluated the robustness and biocompatibility of this electropolymerization-based on-chip valving with a preceding step - dielectrophoretic capture of single melanoma cells within nanoliter-scale chambers. Our results suggest that CPIL can be an excellent candidate as a simple, low-cost and on-demand valve for our single-cell analysis device, and holds potential for application as a structural, extraction, or sensing material in microfluidics.

Electrosynthesis is the production of organic, inorganic, and polymeric materials by electron-transfer reactions at an electrode-electrolyte interface. <sup>7</sup> The use of electricity for synthetic reactions without the need for hazardous chemical oxidants and reductants is recognized as an environmentally benign and cost-effective tool. <sup>8, 9</sup> However, drawbacks still exist in the implementation of electrosynthesis. For example, many organic solvents are poorly conductive or nonconductive, and in such case, large quantities of supporting electrolytes must be employed to promote the ionic current in solution. <sup>10, 11</sup> Furthermore, electrosynthesis is restricted to the electrode surface, and therefore, for preparatory or production-scale applications, mass transfer is an issue. <sup>12</sup> The approach reported here benefits from the high ionic conductivity of an IL and leverages surface confinement of the reaction in conjunction with the high surface-area-to-volume ratio accessible at the microscale to synthesize localized polymer films (plugs) that fill the channel cross section above each electrode in an array of BPEs.

A BPE is a conductor that is immersed in an electrolyte and on which electrically coupled anodic and cathodic reactions proceed simultaneously on opposed extremities (poles) even in the absence of direct ohmic contact. <sup>13-15</sup> This appealing approach relies on the fact that when a conducting object is placed in an electric field applied externally by two driving electrodes, polarization occurs that is proportional to the field strength and the characteristic dimensions of the object. Because no direct electrical connection is required to activate redox reactions, large arrays of BPEs can be controlled with just a single pair of driving electrodes. Bipolar electrochemistry, as a means of electrosynthesis is inherently green, efficient, and sustainable because it requires less supporting electrolyte. <sup>7</sup> Furthermore, the coupled reactions can be utilized to break synthetic symmetry to produce Janus objects. The wireless aspect of BPEs also makes it possible to electrosynthesize and screen novel materials for a wide variety of applications. <sup>16-20</sup>

ILs are organic salts with melting points below 100 °C. They have received considerable attention in recent years because many of their physicochemical properties can be tuned for various applications. Among some of their designed and most exploited properties include tunable

viscosity, large electrochemical window, and good electrical conductivity. <sup>21-23</sup> Furthermore, the introduction of various functional groups into their chemical structures produces compounds that are miscible or immiscible with various organic or aqueous solvent systems. Functionalized ILs can be designed and used as media for specific organic synthesis, as sorbent coatings for solid-phase microextraction, and as solvents for ion-insertion batteries. <sup>23-25</sup> In a previous study by Li et al., <sup>6</sup> the IL 1-decyl-3-methylimidazolium bis[(trifluoromethylsulfonyl)]imide was applied in a microfluidic device to seal nanoliter-scale reaction chambers containing individual tumor cells, to assist in preventing crosstalk during a subsequent bioassay. Compared to other isolation fluids such as mineral oil, <sup>26</sup> the conductivity of ILs allows cells to be lysed electrically by embedded electrodes prior to the assay. However, the low viscosity of the IL in combination with the low interfacial tension at the IL-aqueous boundary led to some intrusion of the IL into the reaction chambers. An ideal IL for this application should be able to maintain a stable boundary at the entrance to each chamber, seal the chamber to prevent crosstalk and evaporation of fluids, and possess moderate viscosity to easily flow into the microfluidic device.

Previous studies have demonstrated the synthesis and design of different types of thiophene- and pyrrole-based ILs for electropolymerization in various applications. <sup>27, 28</sup> Polymer systems generated from thiophene-based IL monomers yielded thermally stable films, while pyrrole-based IL monomers enable the creation of thicker films. Despite these advantages, these compounds are highly viscous and possess high monomer oxidation potentials. Therefore, organic solvent is required as an electrochemical polymerization medium, which limits their application in microfluidic devices, especially in the context of bioanalytical applications.

A new approach to produce intermediate viscosity (less than 500 cP at room temperature), low monomer oxidation potential (as low as 1.4 V vs. Fc<sup>+</sup>/Fc), and solvent-free polymeric ILs for application in microfluidic devices is described herein. A multi-functional CPIL that serves both as the electropolymerizable monomer unit and supporting electrolyte is designed and synthesized. This novel pyrrole-based CPIL can be electrochemically polymerized at controlled potentials to

obtain desired polymer film patterns. The low oxidation potential, moderate viscosity, and resulting film thickness of the pyrrole-based CPIL make it suitable as an on-demand valve in a microfluidic device, even in the presence of an adjacent aqueous phase, as demonstrated in this work. Further, we demonstrate an on-chip valving system can be achieved by rapid growth of CPIL films at selected points within an array of BPEs. This electropolymerization-based on-chip valving uses low voltage (around 5.0 V), a small volume of CPIL monomer (20 µL), and shows high efficiency (simultaneous deposition of 160 polymer films). Importantly, we achieve three polymer film patterns (symmetrical, dissymmetrical, or regional), which are generated under three distinct electric waveform modes with bipolar electrochemistry. The generated polymer films are immobile and sufficiently thick to seal the chambers at room temperature over the duration of our observation window (50 min). Further, the resulting polymer plugs retain their seal even under elevated temperatures that drive evaporation of the aqueous phase from within the chambers. Finally, we show that this method of isolating the chamber with the CPIL and then sealing it with the polymer is compatible with dielectrophoretic capture of melanoma cells in each chamber in preparation for single-cell analysis. This is the first time that hydrophobic ILs are utilized as a functional material for microfluidics, to digitize reaction volumes, and to generate barriers. Significantly, this approach provides a highly conductive alternative material to oils and taps into the tunability of ILs to introduce new research avenues for on-demand coating, valving, extraction and 3D electrodes.

#### **Materials and Methods**

*Materials*. Ethyl acetate (99.8%), hexane (98.5%), dimethyl sulfoxide (99.7%), 1,6-dibromohexane (98%), pyrrole (99%), acetonitrile (99.9%), toluene (99%), dichloromethane (99.9%), potassium hydroxide (98%), ferrocene (98%) and ammonium hexafluorophosphate (99.9%) (NH4PF6) were purchased from Sigma-Aldrich (St. Louis, MO, USA). *N*,*N*-

dimethylformamide (99%) was purchased from Alfa Aesar (Ward Hill, MA, USA). Bis[(trifluoromethylsulfonyl)]imide lithium salt (99%) was purchased from Fisher Scientific (Pittsburgh, PA, USA). 1-methyl-1*H*-imidazole (99%) was obtained from Fluka (Steinheim, Germany). TLC plates with silica gel (60 G F<sub>254</sub>) were obtained from Sigma-Aldrich. Silica gel for column chromatography (230-400 mesh, grade 60) was purchased from Fisher Scientific. All materials were used as received and all organic solvents were dried as needed before use.

Deionized (DI) water (18.2 MΩ cm) was obtained from a Millipore Milli-Q water purification system (Bedford, MA, USA) and used to prepare all aqueous solutions. Bovine serum albumin (BSA) (biotech grade) and 0.25% Trypsin-EDTA (1X) were purchased from Fisher Scientific (Waltham, MA). The DMEM/F12 cell culture medium, dextrose (D-glucose), sucrose, Pluronic F-108 and 1.0 M Tris·HCl stock were obtained from Sigma-Aldrich. The dianionic fluorophore BODIPY<sup>2-</sup> (4, 4-difluoro-1, 3, 5, 7, 8-pentamethyl-4-bora-3a, 4a-diaza-s-indacene-2, 6-disulfonic acid) was obtained from Molecular Probes (Eugene, OR). Low electrical conductivity buffer, which serves as aqueous phase, was comprised of 8.0% sucrose, 0.3% dextrose, and 0.1% BSA in 1.0 mM Tris buffer.

SK-MEL-28 cells were obtained from ATCC and cultured in DMEM/F12 with 10% fetal bovine serum supplementation at 37 °C and 5% CO<sub>2</sub>. In preparation of DEP experiments, SK-MEL-28 cells were detached from culture flask using 0.25% Trypsin-EDTA, followed by pelleting by centrifugation and resuspension in 5.0 mL DEP buffer. Pelleting and resuspension to cell concentration of  $6 \times 10^3$  cells/mL was repeated one additional time to wash cells in DEP buffer before DEP experiments.

Scheme 1 presents the synthetic procedures used to produce the compounds, [pyrrole-C<sub>6</sub>MIm<sup>+</sup>][PF<sub>6</sub><sup>-</sup>] (CPIL1) and [pyrrole-C<sub>6</sub>MIm<sup>+</sup>][NTf<sub>2</sub><sup>-</sup>] (CPIL2) employed in this study, and the corresponding protocols are provided in the *Supporting Information*. The purity of compounds **2**-5 was verified using <sup>13</sup>C and <sup>1</sup>H NMR, and all spectra can be found in the *Supporting Information*.

Instrumentation. For the characterization of all synthesized compounds, a Varian MR-400 nuclear magnetic resonance (NMR) spectrometer was used.  $^{1}$ H and  $^{13}$ C chemical shifts are expressed in parts per million (ppm,  $\delta$ ), downfield from tetramethylsilane (TMS) ( $\delta = 0$  ppm) by using the signals of the residual protons of the following deuterated solvents at room temperature: chloroform- $d_{1}$  (7.26 ppm for  $^{1}$ H and 77.0 ppm for  $^{13}$ C spectra) and DMSO- $d_{6}$  (2.50 ppm for  $^{1}$ H and 39.5 ppm for  $^{13}$ C spectra). For high-resolution mass spectrometry, an Agilent Technologies 6230B Accurate Mass Time of Flight mass spectrometer with an electrospray source was used.

The viscosity of pyrrole-based IL monomers was measured by Brookfield DV1 cone (AMETEK Brookfield, MA) and plate viscometer with a CPA-51Z cone spindle at 20 °C. Optical microscopy images of sealing properties and thickness of polypyrrole-based IL films were obtained using Nikon eclipse Ti inverted microscope and Nikon AZ-100 microscope (Nikon, Tokyo, Japan), respectively.

Electrochemical studies were performed with a CH Instruments Potentiostat (750E Series, Austin, TX) by using a three-electrode electrochemical cell. An unmodified platinum electrode (Bioanalytical System, Inc., MF-2113) served as the working electrode. The auxiliary electrode was platinum mesh. A 0.5-mm diameter platinum wire and ferrocene, added to the solution phase, acted as a pseudoreference electrode. Deoxygenation was conducted by nitrogen purging before the electrochemical experiments. CPIL was vacuumed under the Schlenk line for 30 minutes before making the solution.

Electropolymerization of pyrrole-based IL monomers were performed under direct current (DC) or alternating current (AC) voltage to achieve the dissymmetrical or regional polymer film patterns. DC power was supplied to driving electrodes using a BK Precision 1687B power supply (Melrose, MA), while AC power was provided by a Tektronix AG3011C waveform generator (Tektronix, Beaverton, OR).

Voltammetric characterization of the electropolymerization of ionic liquids from solution. The working electrode was an unmodified 3.0-mm diameter Pt electrode, a Pt mesh was used as auxiliary electrode, and a 0.5-mm diameter Pt wire with added 6.0 mM ferrocene provided a reference potential. First, the Pt working electrode was polished with alumina (5.0 mm, 0.3 mm, 0.05 mm), and then was sonicated in DI water for 3 min and ethanol for 2 min (Branson model 1210 ultrasonic bath) each time. The electrode was pretreated by cycling its potential in a 0.5 M H<sub>2</sub>SO<sub>4</sub> solution until a constant cyclic voltammogram (CV) appeared. The electrode was then washed with DI water and ethanol, dried, and placed in a 3.0-mL acetonitrile solution containing 30 μL CPIL monomer (44.4 mg) and 6.0 mM ferrocene. Electropolymerization was performed at 50 mV/s by cycling the potential of the working electrode from -2.8 V to 2.0 V versus Fc<sup>+</sup>/Fc. Finally, the electrode was removed and rinsed with DI water for further experimentation. The electrodes were evaluated by bright field microscopy (Nikon AZ100, Nikon Co., Tokyo, Japan) to confirm deposition of the polymer film.

Device fabrication and operation. Standard photolithography and etching processes were used to fabricate the microfluidic device. First, the electrode design was patterned using a positive photoresist (AZ P4620; MicroChemicals GmbH, Ulm, Germany) on Au-coated glass (5 nm-thick Cr adhesion layer and 100 nm-thick Au top layer, EMF Corp., Ithaca, NY). The slides were developed by AZ 400K developer, followed by wet etching the Au (KI:  $I_2$ :  $H_2O = 4.0$  g: 1.0 g: 40.0 mL) and then the Cr (chromium etchant; Sigma Aldrich, St. Louis, MO). 1-methyl-2-pyrrolidone (NMP) was employed to dissolve the remaining photoresist. Finally, the electrodes were rinsed with pure anhydrous ethanol (200 proof) and dried under a stream of  $N_2$ .

Second, channel molds were patterned using negative photoresist (SU-8 2025, Microchem Corp., Westborough, MD) on a Si substrate. Subsequently, the poly(dimethylsiloxane) (PDMS, Sylgard 184 elastomer kit, Dow Corning Corp., Midland, MI) precursor was poured onto the SU-8 mold and cured at room temperature for 5 days (to prevent shrinking after release from the mold).

The alignment of PDMS microchannels with BPE array electrodes was carried out using the following procedure. First, the slides with electrode pattern and PDMS channels were exposed to an air plasma (Plasma cleaner, Harrick Scientific, Ithaca, NY) for 60 s to activate the surfaces for permanent bonding. Second, a few drops of ethanol were applied on both surfaces to delay bonding and to facilitate alignment. Third, the aligned device was baked at 65 °C overnight to completely drive off the ethanol and to encourage bonding. Finally, 3.0 µM Pluronic in 1.0 mM DEP buffer was injected into the device (following evacuation of entrapped air from the device under vacuum) and kept at 4 °C overnight to coat the channel surface. After coating with Pluronic, all channels were rinsed with DEP buffer for 20 min before experiments.

The dimensions of the microfluidic device included four microchannels, each being 7.0 mm long  $\times$  110  $\mu$ m wide  $\times$  25  $\mu$ m tall arranged in parallel. Each channel had 20 chambers along each side (total 160 chambers). Each chamber was circular with a diameter of 110  $\mu$ m, and connected to the channel by a 20  $\mu$ m  $\times$  20  $\mu$ m opening, with a leak channel (7  $\mu$ m wide) affixed to each chamber to make a fluidic connection to the main channel. The picture of the device is shown in Scheme 2a. Biopsy punches were used to create 3.0 mm-diameter inlet and 1.0 mm-diameter outlet reservoirs. Two BPE designs were employed in this study. The "continuous" BPEs (16  $\mu$ m wide  $\times$  7  $\mu$ m tall) extended into the chambers from under the PDMS to a distance of 3.0  $\mu$ m from the channel (Scheme 2a and 2b). The "notched" BPEs narrowed to a 5.0  $\mu$ m-wide waist at the center of each chamber to create a local electric field maximum that can be utilized for recapture of the cells by positive DEP. The electrodes comprising each of the two outermost rows were interconnected to form "driving electrodes" and led to contacts for the power supply.

Fluid isolation and electropolymerization in the BPE array-based microfluidics. Following pretreatment with Pluronic, devices were rinsed with DEP buffer for 20 min. Then, 0.25 mM BODIPY<sup>2-</sup> in DEP buffer was introduced at 2.0 μL/min for 15 min, followed by introduction of 20 μL of neat CPIL monomer at 200 nL/min. Once the CPIL reached the end of the device, the flow

rate was reduced to 20 nL/min, a DC or AC voltage (as detailed in each subsection of the Results and Discussion) was applied to the driving electrode contacts for 5 min to conduct electropolymerization. A microscope (Nikon AZ100, Nikon Co., Tokyo, Japan) and a sCMOS camera (Andor Zyla 4.2, Oxford Instruments, Abingdon, Oxfordshire, England) were used to observe the pattern of the resulting polymer film.

A DC power supply was utilized for dissymmetrical electropolymerization (mode 2). In this scenario, 5.0 V was applied between driving electrodes, and after 5 min, the DC voltage was turned off.

AC power was supplied to the driving electrodes to generate 2D or 1D arrayed polymer film patterns. To obtain a 2D-array symmetrical polymer film pattern, an alternating square wave (6  $V_{pp}$ , 500 mHz) was applied for 5 min (mode 1). To obtain a 1D-array regional polymer film pattern, an alternating current sine wave (1  $V_{pp}$ , 1 Hz, DC offset = 2 V) was applied for 5 min (mode 3). Scheme 3 illustrate electropolymerization in the microfluidic device under three modes.

In an experiment to test the robustness of the seal provided by the polymer film under conditions conducive to evaporation, the device was first filled with DEP buffer. Then, the CPIL was flowed into the channels at 200 nL/min, thereby digitizing the aqueous chamber volumes. The CPIL was polymerized under mode 1. Finally, the device was mounted on the Tokai Hit TPi-W thermal stage with setting temperature (37 °C), and the sealing property was observed under microscope for 25 min.

Dielectrophoretic capture of melanoma cells. This device dimensions are suitable to capture melanoma cells (SK-MEL-28) individually at the BPE tips aligned to the entrance of each chamber following our previously published method.<sup>6</sup> Scheme 2c-f illustrate the workflow of on-chip valving. Briefly, the device was first rinsed with DEP buffer (around 75.68  $\mu$ S/cm) at a flow rate of 200 nL/min for 20 min. Second, 20  $\mu$ L of a suspension of cells in DEP buffer was flowed into the device at 200 nL/min, and an AC voltage (16 V<sub>pp</sub>) was applied at the coplanar driving

electrodes at each side of the BPE array a Tektronix AFG3011C waveform generator. The AC frequency was maintained at 50 kHz at which these melanoma cells experienced strong positive DEP (are attracted toward higher electric field strength). Within this 20 min time period, approximately 25 cells were introduced into the device. Third, the AC voltage was turned off, which allows for cells captured at the BPE tips to be transferred hydrodynamically into the chambers. Fourth, the cell suspension in the inlet reservoir was exchanged for DEP buffer only. Flowing the DEP buffer for 10 min at 200 nL/min pushed each cell further into the chamber until each stopped at the entrance to the 'leak' channel (the narrow sigmoidal channel that interconnects the chamber to the main channel to allow for fluid circulation). Then, the CPIL was added and flowed into the channels at the same flow rate. When the CPIL reached to the end of the device, the waveform generator was turned on (6 V<sub>pp</sub>, 500 mHz) and was applied for 5 min (mode 1). Nikon AZ-100 microscope (Nikon, Tokyo, Japan) were utilized to image cells to obtain fluorescence and optical images.

Simulation of the electric field distribution within the BPE array. A parallel-channel model coupled with BPEs to shape the electric field was simulated and investigated using the steady-state finite element method (COMSOL Multiphysics 5.6). In this design, appropriate physical constants were used to represent gold BPEs, PDMS, molten salt, and DEP buffer. Details of the simulation conditions are available in the Supporting Information). In the simulation, the dimensions (e.g., channel width, chamber size and BPE tip position and shape) matched those of devices employed in the experiments. The distribution of the electric field is shown for the continuous BPE and notched BPE designs in Figure 1a and Figure 1d, respectively. Figure 1b,e are line plots the electric field strength along cutlines bisecting a row of BPEs in each of these configurations. The maximum electric field strength is located at the BPE tips and is approximately 13.8 kV/m for the parallel-channel design. A plot of the electric potential is shown in Figure 1c,f.

### **Results and Discussion**

Synthesis and properties of ionic liquids. Two pyrrole-based IL monomers, shown in Scheme1, were synthesized in this study. The synthesis of two N-substituted pyrrole-based IL monomers (CPIL1 and CPIL2) was carried out according to a previously reported synthetic route <sup>27</sup> to obtain CPIL1 followed by exchange of the [PF6<sup>-</sup>] anion to the [NTf2<sup>-</sup>] anion to form CPIL2. Scheme 1 summarizes the synthesis of these two CPILs. First, pyrrole (1) was reacted and coupled with 1,6-dibromohexane to obtain compound 2. This alkylation was performed under the controlled addition of reactants and dilute conditions to avoid dimerization. Afterward, the resulting product was transformed into the pyrrole functionalized imidazolium salt (3). In the final step, the exchange of the [Br<sup>-</sup>] anion with NH<sub>4</sub>PF<sub>6</sub> or LiNTf<sub>2</sub> afforded the monomers as the [PF6<sup>-</sup>] or [NTf2<sup>-</sup>] salts, respectively.

The viscosity of ILs is an important feature that often dictates their use in many applications as it is known to affect the mass-, heat- and electron-transfer rates and flow behavior.  $^{29,30}$  Low viscosity ILs are useful in applications requiring fluid manipulation, especially in microfluidic devices. In this study, a syringe pump was employed to manipulate fluid flow. Based on Hagen-Poiseuille equation, fluid pressure drop dP is proportional to both the mean flow rate, Q, and fluidic resistance, R. All viscosities and densities of ILs were measured at a temperature of 20 °C. CPIL1 was observed to have a viscosity 682 cP and have a density 1.55 g/cm<sup>3</sup>, after exchange of the anion from [PF6<sup>-</sup>] to [NTf2<sup>-</sup>], the viscosity of CPIL2 decreased to 363 cP and density drop to 1.48 g/cm<sup>3</sup>. Among these two CPILs, CPIL2 possessed a lower viscosity and was anticipated to be suitable for applications requiring fluid manipulation, such as microfluidics. Given the viscosities and the dimensions of the bifurcated 4-channel device, the hydraulic resistance of CPIL2 in each channel is  $1.77 \times 10^{16}$  Pa·s/m<sup>3</sup>, and  $3.33 \times 10^{16}$  Pa·s/m<sup>3</sup> for CPIL1. Therefore, CPIL2 requires 2.13 psi  $(1.47 \times 10^2 \text{ mBar})$  to achieve the flow rate (Q = 50 nL/min). However, CPIL1 requires 4.03 psi

 $(2.78 \times 10^2 \text{ mBar})$  to generate the same flow rate. Because of the high viscosity of CPIL1, it was difficult to introduce the IL into the microfluidic device at a constant rate.

Electrochemical characterization. The electrochemical behavior of CPIL2 was examined systematically by cyclic voltammetry. In each experiment, two voltammetric scans were obtained at a fixed scan rate of 50 mV s<sup>-1</sup> at a Pt working electrode, and the first scan is shown in Figure 2 A freshly prepared solution was utilized for each voltammetric trial. First, a cyclic voltammogram (CV) was obtained in 6.0 mM ferrocene in CH<sub>3</sub>CN to serve as a background. Second, to account for the effect of an electrolyte, 105 mM NH<sub>4</sub>PF<sub>6</sub> and 6.0 mM ferrocene in CH<sub>3</sub>CN was evaluated. Finally, the CPIL was added in CH<sub>3</sub>CN with volumetric ratio of 1:100 (29.0 μM), and CVs were obtained under two conditions, with and without ferrocene. Figure 2 shows the voltammetric response obtained for CPIL2.

To understand the electrochemical behavior of the CPIL, it is helpful to first revisit the electrochemical polymerization of pyrrole based on Diaz's mechanism.  $^{31, 32}$  The removal of an electron from pyrrole forms a reactive radical cation. This radical cation reacts with a second radical cation to form the dihydromer dication, and the loss of two protons forms the aromatic dimer. The dimer grows by the addition of more such units at the  $\alpha$  position, to form oligomeric products and then the polymer. The extended conjugation in the polymer results in a lowering of the oxidation potential compared to the monomer. The anion is incorporated into the polymer to ensure the electrical neutrality of the film, and at the end of the reaction, a polymeric film of controllable thickness is formed at the anode.

The primary wave of the CV is an irreversible anodic peak corresponding to the removal of an electron from the HOMO of the electron-rich  $\pi$ -system. In the initial scan of CPIL2 in CH<sub>3</sub>CN, the electropolymerization of CPIL2 occurs at 1.394 V vs. Fc<sup>+</sup>/Fc. The electrochemical potential window observed for the solvent and the anion [NTf<sub>2</sub>-] agrees with a previous study, <sup>22</sup> that

bis(triflyl)amides are not oxidized before 2.0 V vs. I<sup>-</sup>/I<sub>3</sub><sup>-</sup>. The I<sup>-</sup>/I<sub>3</sub><sup>-</sup> couple has a measured potential of -0.195 V vs. ferrocene/ferrocenium in the ([EtMeIm<sup>+</sup>][NTf<sub>2</sub><sup>-</sup>]) IL.

Symmetrical deposition of CPIL at a BPE array in a multichannel device (mode 1). Having characterized the electrochemical properties of CPIL2, we next evaluated its performance in the intended application: on-demand valving of microchambers in our single-cell analysis device. A multichannel microfluidic device was used to perform the electrodeposition of neat CPIL2. An aqueous solution (DEP buffer) was introduced into the device until all the chambers and channels were filled. Next, 20 µL of neat CPIL2 was pipetted into the inlet reservoir and subsequently introduced into the device under negative pressure at a flow rate 200 nL/min. As shown in Video S1, upon its introduction into the device, the CPIL forms a stable fluid boundary and is immiscible with the DEP buffer. Once the CPIL reached the outlet, the flow rate was reduced to 20 nL/min. Finally, a square wave voltage was applied between the two driving electrodes (Video S1). At an amplitude of 4 V (alternatively stepping from -2 V to 2 V, t = 45 s in Video S1), a polymer film formed over a period of 5 min at the tips of the driving electrodes, which were aligned to the openings of the chambers in the outermost rows. When the amplitude was increased to 6 V (stepping from -3 V to 3 V, t = 70 s in Video S1), the polymer was formed at all the openings. After 5 min, no further growth in film thickness was observed. The polymer film pattern under this mode (mode 1, Figure 3d) is symmetrical as shown in Figure 3a.

Symmetrical deposition of the CPIL film is attributed to the bimodal function of BPEs under an alternating electric field; each BPE tip functions alternately as an anode and cathode. At a BPE anode in contact with the CPIL monomer, electropolymerization occurs when a sufficient interfacial potential develops in response to an applied voltage. The interfacial potential at the driving electrodes is higher than at the remainder of the array (BPEs), and therefore, at the lower amplitude (4 V), film formation is exclusive to these outermost rows. At the higher amplitude (6 V), the entire array is supplied with sufficient overpotential to drive electropolymerization.

This result is significant because, under the conditions employed, the CPIL film is formed symmetrically (on both sides of each channel) at the opening to all the chambers in the array. This pattern is beneficial for sealing the chambers, isolating their contents, which is useful for single-cell analysis. Such on-demand CPIL structures hold potential for other applications related to analysis (e.g., sensing or extraction). These applications are the focus of ongoing research in our laboratories. Deposition of the CPIL film at only the driving electrodes creates the opportunity to selectively address only the outermost rows of chambers. This outcome is potentially useful for incorporating a row of controls or for building systems that evaluate communication between distinct cell types. The following section discusses two further selective modes of electropolymerization.

Dissymmetrical and selective deposition of neat CPIL (mode 2 and mode 3). We next evaluated voltage patterns that were selected to break symmetry, yielding CPIL films on only one side of each channel and then, at only one row in the device. In these experiments, the device was filled with DEP buffer and then CPIL monomer using the same protocol as was described in the preceding section.

Dissymmetrical electropolymerization of the CPIL was accomplished by the application of DC voltage. Figure 3b and Figure 3e show the dissymmetrical CPIL film pattern and applied waveform, respectively. These results show that under 5 V, CPIL monomers were electropolymerized at the anodic BPE tips. Previously, Koizumi et al. have reported the DC-bipolar electropolymerization of PEDOT and pyrrole on gold electrodes. <sup>19</sup> The corresponding polypyrrole films were prone to deposit on the anode, and the films were confined to the surface of the electrode instead of growing a polypyrrole fiber. Our result also confirmed that CPIL films were deposited at the opening to one side of the chambers in the array, and while the chamber openings were filled (occluded) by the film, the polymer did not extend into the channel.

Regional electropolymerization of the CPIL was achieved by application of an AC voltage with a DC offset, instead of alternating equally above and below zero volts. The voltage was varied between +2.5 V and +1.5 V. This setting has an offset of 2.0 V and a frequency of 1 Hz, which can be presented as  $v_t = \sin(2\pi t) + 2$  and the waveform shown in Figure 3f. By using this waveform, the CPIL films were deposited at the openings of the outermost chambers on only one side of the device, as shown in Figure 3c. This regional polymer film pattern suggested a 1D polymer film array could be selectively patterned first, and shows application of the breaking of symmetry.

These two patterns (dissymmetrical and regional) demonstrate control over the location of electropolymerization in a microfluidic device for on-demand valving, and the polymer film patterns can be generated rapidly (within 5 min).

CPIL as an on-demand valve to seal microchambers. We next evaluated the ability of the CPIL polymer film to form a stable microstructure and to act as a seal or valve. To aid in the evaluation of the CPIL as a seal, BODIPY<sup>2-</sup> was added into the DEP buffer so that the aqueous phase could be clearly distinguished by fluorescence microscopy. As in experiments discussed in the preceding sections, the device was first filled with the aqueous phase followed by flowing the CPIL into the device to displace the fluorescent solution in the microchannels only. As before, the CPIL formed immiscible phase boundary with the fluorescent aqueous phase at each chamber opening. A recording of the introduction of CPIL is provided in Video S2. The CPIL was then polymerized under mode 1. After electropolymerization for 5 min, the waveform generator was turned off, and the flow rate was maintained at 20 nL/min for 50 min. The phase boundary was observed by fluorescence microscopy at the conclusion of electropolymerization (t = 0 min) and at t = 15 min and t = 50 min. A control experiment was performed under matched condition without electropolymerization. Electropolymerization of CPIL2 was also tested in a distinct microfluidic

device (rectangular chamber) design with mode 2, and dissymmetrical polymer film pattern formed as shown in Video S3.

Figure 4 shows images obtained in the absence (Figure 4c,d) and presence (Figure 4a,e,f) of electropolymerization. Without polymerization, an unstable and mobile boundary was observed. The immiscible boundary was expanded over the 50 min period of observation, and the CPIL2 monomer intruded into the chambers, occupying about 25% of the chamber volume. However, the polymer-sealed chambers maintained a stable and immobile boundary in the observation window (50 min). Polymerization of the CPIL monomers successfully immobilized them, and the thickness of the polymer films was sufficient to seal the chamber openings.

We further evaluated the robustness of the seal under conditions relevant to single-cell enzymatic assay. A separate device was filled with DEP buffer and sealed with polymer films using mode 1 as described in the preceding subsections. Then, the device was subjected to an elevated temperature (37 °C) on a heated stage for 25 min. During this time, a fraction of the aqueous volume in the chambers evaporated owing to the gas permeability of PDMS. The phase boundaries between the water, CPIL, and polymer were monitored by microscopy. Figure 5 shows brightfield micrographs obtained for two chambers at three time points each. The CPIL-water boundary (indicated by red arrows, Figure 5) was observed to progress through the leak channel towards the chamber due to the negative pressure generated in the chambers by evaporation. However, the polymer films remained stable, and CPIL did not leak past, indicating that the polymer provides a robust seal.

These findings, suggest that CPIL can be introduced into a microfluidic device, electropolymerized to form films in a controlled pattern and immobilized to create a permanent structure such as a robust barrier or seal. Based on these results, CPIL is an excellent candidate as an on-demand valve for our single-cell analysis device and holds potential for applications as a structural, extraction, or sensing material to be deposited within microfluidic devices.

Isolation of individually captured melanoma cells by CPIL electropolymerization. To further evaluate the biocompatibility of this electropolymerization-based on-chip valving, we introduced melanoma cells, as model CTCs, into the microfluidic device and captured them at the entrance to each chamber using dielectrophoresis (DEP) following the procedure described in the *Materials and Methods* section. Briefly, the cells were flowed into the device at a constant flow rate of 200 nL/min and captured at the BPE tips when the AC capture voltage (16 V<sub>pp</sub> at 50 kHz) was applied. Then, the AC capture voltage was turned off. When AC voltage was off, the captured cells began to release from the BPE tips and transferred into the reaction chambers. This occurs because in the absence of the external electric field, the cell is carried into the chamber by drag force towards the chamber generated by circulation of the DEP buffer into the chamber entrance and out of the sigmoidal leak channel.

Following cell transfer into the chambers, the CPIL was added and flowed into the channels. A clear boundary between the CPIL and aqueous buffer in chambers was formed. Once the CPIL reached the end of the device, a square wave voltage was applied (mode 1) to drive polymerization. The CPIL was electropolymerized at the opening of the chambers as shown in Figure 6, and the cells were not disturbed during this proces. This result shows that electropolymerization-based on-chip valving is compatible with isolation of individual tumor cells by DEP.

#### **Conclusions**

Two room temperature CPILs with pyrrole functional groups were synthesized, and their physicochemical properties characterized. The monomeric form of CPIL2 has sufficiently low viscosity and high hydrophobicity to fill a microchannel under low pressure (less than 2 psi), thereby digitizing the aqueous sample phase within the chambers. Cyclic voltammetry has been used to examine the electrochemical activity of CPIL2 and shows its oxidation potential to be 1.4 V vs. Fc<sup>+</sup>/Fc. This low oxidation potential allowed for homogeneous electropolymerization of this

IL in a microfluidic device prefilled with an aqueous phase. The formed films of pyrrole-based IL were immobile and maintained a stable phase boundary during an observation window of 50 min. Furthermore, by tuning the electric waveform, three distinct polymer film patterns were achieved, which allows for controlled placement of the film and in this application, for valving of selected microchambers.

Electropolymerization of the CPIL in our microfluidic device requires a low voltage (around 5.0 V), consumes a small volume of monomer (20 μL), and shows high efficiency (160 polymer depositions). The polymer films at the BPE tips resulted in a solid plug that defines a stable phase boundary over durations relevant to a nucleic acid or enzymatic assay and remains in place despite evaporation of the aqueous contents of the chambers at elevated temperature. Finally, this method is compatible with DEP-based capture of individual melanoma cells, which indicates its potential as a seal in single-cell assays. This advancement is innovative in that hydrophobic ILs have not been utilized as a functional material for microfluidics, to digitize reaction volumes, or to generate barriers in this context. Significantly, this approach provides a highly conductive alternative material to oils and taps into the tunability of ILs to introduce new research avenues for on-demand coating, valving, extraction and 3D electrodes.

Our ongoing research will identify conditions for electropolymerization at BPEs with an additional gap in the chambers (our previously reported "split BPE" configuration),<sup>6</sup> which allows for cell recapture and electrical lysis. Our preliminary results indicate that water electrolysis, which leads to undesirable gas bubble formation, occurs within this gap to complete the circuit, thereby providing sufficient current for electropolymerization. Therefore, we anticipate that a sacrificial redox agent will be required as an additive in the aqueous phase. In subsequent studies, we also aim to exploit this electropolymerization-based on-chip valving to accomplish a variety of molecular analyses of individual cells.

## Acknowledgement

Research in this manuscript was supported by the National Institutes of Biomedical Imaging and Bioengineering of the National Institutes of Health under award number 5R21EB028583 and by the Chemical Measurement and Imaging Program at the National Science Foundation (Grant No. CHE-1709372).

# **Brief description of the supplementary material**

The supplementary material provides the synthetic protocols of compound **2-5**. The proton NMR for all synthesized compounds and the carbon NMR for **CPIL1** and **CPIL2** have been shown. Two-dimensional numerical simulation of the open-channel and the parallel-channel have been plotted. Videos of electropolymerization in two microfluidics and isolation of **CPIL2** have been provided.

## Reference

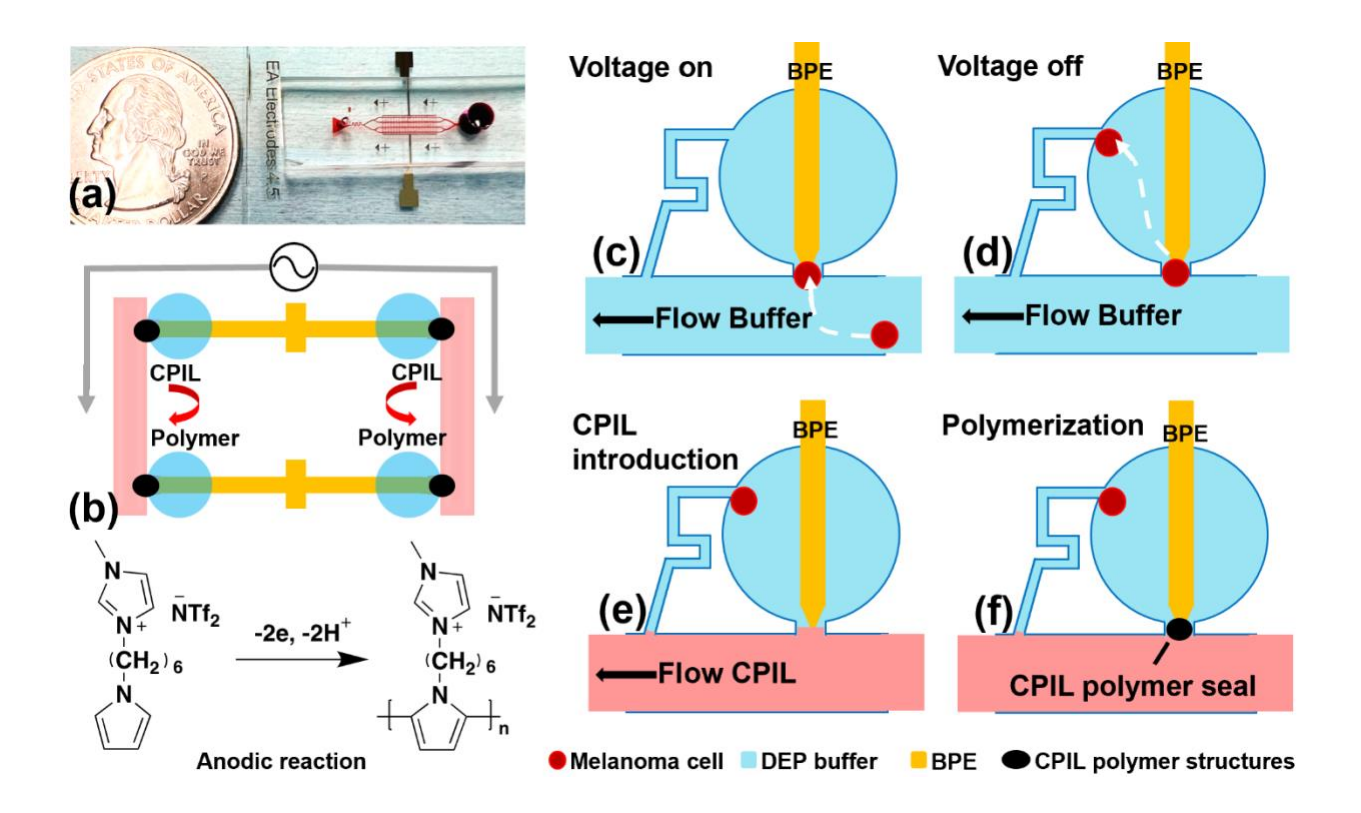
- 1. Marusyk, A.; Polyak, K., Tumor heterogeneity: Causes and consequences. *Biochimica et Biophysica Acta (BBA) Reviews on Cancer* **2010,** *1805* (1), 105-117.
- 2. Reya, T.; Morrison, S. J.; Clarke, M. F.; Weissman, I. L., Stem cells, cancer, and cancer stem cells. *Nature* **2001**, *414* (6859), 105-111.
- 3. Chaffer, C. L.; Weinberg, R. A., A Perspective on Cancer Cell Metastasis. *Science* **2011**, *331* (6024), 1559-1564.
- 4. Cristofanilli, M.; Budd, G. T.; Ellis, M. J.; Stopeck, A.; Matera, J.; Miller, M. C.; Reuben, J. M.; Doyle, G. V.; Allard, W. J.; Terstappen, L. W. M. M.; Hayes, D. F., Circulating Tumor Cells, Disease Progression, and Survival in Metastatic Breast Cancer. *New England Journal of Medicine* **2004**, *351* (8), 781-791.
- 5. Nagrath, S.; Sequist, L. V.; Maheswaran, S.; Bell, D. W.; Irimia, D.; Ulkus, L.; Smith, M. R.; Kwak, E. L.; Digumarthy, S.; Muzikansky, A.; Ryan, P.; Balis, U. J.;

- Tompkins, R. G.; Haber, D. A.; Toner, M., Isolation of rare circulating tumour cells in cancer patients by microchip technology. *Nature* **2007**, *450* (7173), 1235-9.
- 6. Li, M.; Anand, R. K., Integration of marker-free selection of single cells at a wireless electrode array with parallel fluidic isolation and electrical lysis. *Chemical Science* **2019**, *10* (5), 1506-1513.
- 7. Shida, N.; Zhou, Y.; Inagi, S., Bipolar Electrochemistry: A Powerful Tool for Electrifying Functional Material Synthesis. *Accounts of Chemical Research* **2019**, *52* (9), 2598-2608.
- 8. Nezakati, T.; Seifalian, A.; Tan, A.; Seifalian, A. M., Conductive Polymers: Opportunities and Challenges in Biomedical Applications. *Chem Rev* **2018**, *118* (14), 6766-6843.
- 9. Yoshida, J.-I.; Kataoka, K.; Horcajada, R.; Nagaki, A., Modern Strategies in Electroorganic Synthesis. *Chemical Reviews* **2008**, *108* (7), 2265-2299.
- 10. Yuan, Y.; Lei, A., Is electrosynthesis always green and advantageous compared to traditional methods? *Nature Communications* **2020**, *11* (1).
- 11. Beil, S. B.; Pollok, D.; Waldvogel, S. R., Reproducibility in Electroorganic Synthesis—Myths and Misunderstandings. *Angewandte Chemie International Edition* **2021**, *60* (27), 14750-14759.
- 12. Stalder, R.; Roth, G. P., Preparative Microfluidic Electrosynthesis of Drug Metabolites. *ACS Medicinal Chemistry Letters* **2013**, *4* (11), 1119-1123.
- 13. Fosdick, S. E.; Knust, K. N.; Scida, K.; Crooks, R. M., Bipolar Electrochemistry. *Angewandte Chemie International Edition* **2013**, *52* (40), 10438-10456.
- 14. Mavré, F.; Anand, R. K.; Laws, D. R.; Chow, K.-F.; Chang, B.-Y.; Crooks, J. A.; Crooks, R. M., Bipolar Electrodes: A Useful Tool for Concentration, Separation, and Detection of Analytes in Microelectrochemical Systems. *Analytical Chemistry* **2010**, *82* (21), 8766-8774.
- 15. Rahn, K. L.; Anand, R. K., Recent Advancements in Bipolar Electrochemical Methods of Analysis. *Analytical Chemistry* **2021**, *93* (1), 103-123.
- 16. Loget, G.; Roche, J.; Kuhn, A., True Bulk Synthesis of Janus Objects by Bipolar Electrochemistry. *Advanced Materials* **2012**, *24* (37), 5111-5116.
- 17. Loget, G.; Kuhn, A., Bulk synthesis of Janus objects and asymmetric patchy particles. *Journal of Materials Chemistry* **2012**, *22* (31), 15457.

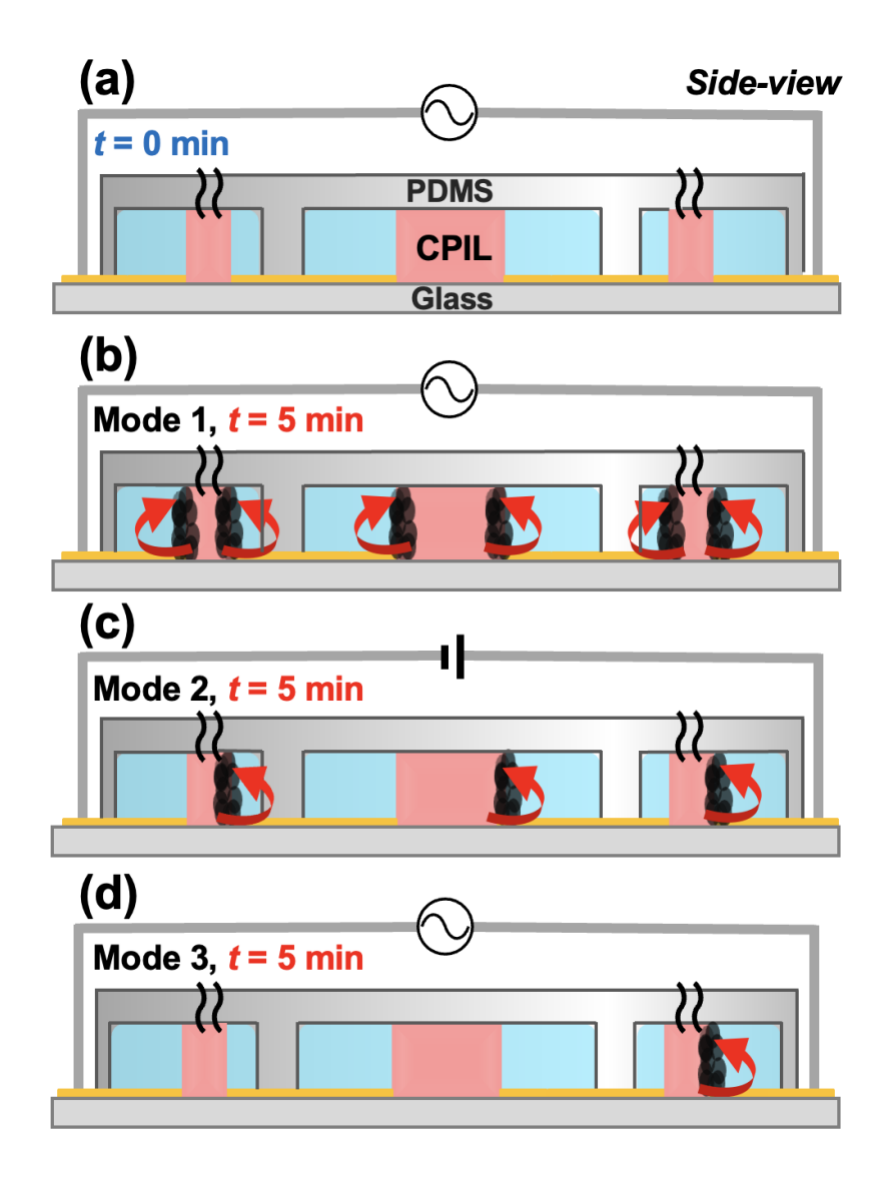
- 18. Shida, N.; Koizumi, Y.; Nishiyama, H.; Tomita, I.; Inagi, S., Electrochemically mediated atom transfer radical polymerization from a substrate surface manipulated by bipolar electrolysis: fabrication of gradient and patterned polymer brushes. *Angew Chem Int Ed Engl* **2015**, *54* (13), 3922-6.
- 19. Koizumi, Y.; Shida, N.; Ohira, M.; Nishiyama, H.; Tomita, I.; Inagi, S., Electropolymerization on wireless electrodes towards conducting polymer microfibre networks. *Nature Communications* **2016**, *7* (1), 10404.
- 20. Inagi, S., Site-selective anisotropic modification of conductive objects by bipolar electropolymerization. *Polymer Journal* **2019**, *51* (10), 975-981.
- 21. Ding, J.; Zhou, D.; Spinks, G.; Wallace, G.; Forsyth, S.; Forsyth, M.; Macfarlane, D., Use of Ionic Liquids as Electrolytes in Electromechanical Actuator Systems Based on Inherently Conducting Polymers. *Chemistry of Materials* **2003**, *15* (12), 2392-2398.
- 22. Bonhôte, P.; Dias, A.-P.; Papageorgiou, N.; Kalyanasundaram, K.; Grätzel, M., Hydrophobic, Highly Conductive Ambient-Temperature Molten Salts. *Inorganic Chemistry* **1996**, *35* (5), 1168-1178.
- 23. Yu, H.; Ho, T. D.; Anderson, J. L., Ionic liquid and polymeric ionic liquid coatings in solid-phase microextraction. *TrAC Trends in Analytical Chemistry* **2013**, *45*, 219-232.
- 24. Shimizu, M.; Usui, H.; Sakaguchi, H., Functional ionic liquids for enhancement of Liion transfer: the effect of cation structure on the charge—discharge performance of the Li4Ti5O12 electrode. *Physical Chemistry Chemical Physics* **2016**, *18* (7), 5139-5147.
- 25. Li, D.; Shi, F.; Peng, J.; Guo, S.; Deng, Y., Application of Functional Ionic Liquids Possessing Two Adjacent Acid Sites for Acetalization of Aldehydes. *The Journal of Organic Chemistry* **2004**, *69* (10), 3582-3585.
- 26. Cohen, D. E.; Schneider, T.; Wang, M.; Chiu, D. T., Self-Digitization of Sample Volumes. *Analytical Chemistry* **2010**, *82* (13), 5707-5717.
- 27. Devasurendra, A. M.; Zhang, C.; Young, J. A.; Tillekeratne, L. M. V.; Anderson, J. L.; Kirchhoff, J. R., Electropolymerized Pyrrole-Based Conductive Polymeric Ionic Liquids and Their Application for Solid-Phase Microextraction. *ACS Applied Materials & Interfaces* **2017**, *9* (29), 24955-24963.

- 28. Young, J. A.; Zhang, C.; Devasurendra, A. M.; Tillekeratne, L. M.; Anderson, J. L.; Kirchhoff, J. R., Conductive polymeric ionic liquids for electroanalysis and solid-phase microextraction. *Anal Chim Acta* **2016**, *910*, 45-52.
- 29. Hallett, J. P.; Welton, T., Room-Temperature Ionic Liquids: Solvents for Synthesis and Catalysis. 2. *Chemical Reviews* **2011**, *111* (5), 3508-3576.
- 30. Seddon, K. R.; Stark, A.; Torres, M.-J., Influence of chloride, water, and organic solvents on the physical properties of ionic liquids. *Pure and Applied Chemistry* **2000**, *72* (12), 2275-2287.
- 31. Diaz, A. F.; Kanazawa, K. K.; Gardini, G. P., Electrochemical polymerization of pyrrole. *Journal of the Chemical Society, Chemical Communications* **1979**, (14), 635.
- 32. Sabouraud, G.; Sadki, S.; Brodie, N., The mechanisms of pyrrole electropolymerization. *Chemical Society Reviews* **2000**, *29* (5), 283-293.

**Scheme 1.** Synthetic procedure used to prepare the N-substituted pyrrole-based imidazolium CPILs evaluated in this study.



**Scheme 2.** Schematic overview of (a) the microfluidic chip and (b) electropolymerization of CPIL at BPE tip. (c-f) Illustration of the workflow of on-chip valving, which includes (c) capturing single melanoma cells by DEP, (d) hydrodynamic transfer of a captured cell to the leak channel (DEP off), (e) introduction of CPIL into the main channel, and (f) electropolymerization of CPIL and formation of the seal.



Scheme 3. Illustration of the three polymer film patterns (symmetrical, dissymmetrical, or regional) modes of electro deposition of neat CPIL2 in the multi-channel microfluidic device. (a) shows CPIL monomer was introduced into the microfluidic device and formed immiscible phase with the buffer. (b) shows symmetrical polymer films pattern (mode 1) was achieved by using alternating square wave. (c) shows dissymmetrical polymer films pattern (mode 2) was reached by using DC power supply. (d) shows regional polymer films pattern (mode 3) was generated by using AC voltage with a DC offset. A movie showing the entire experiment is provided in the *Supporting Information*.

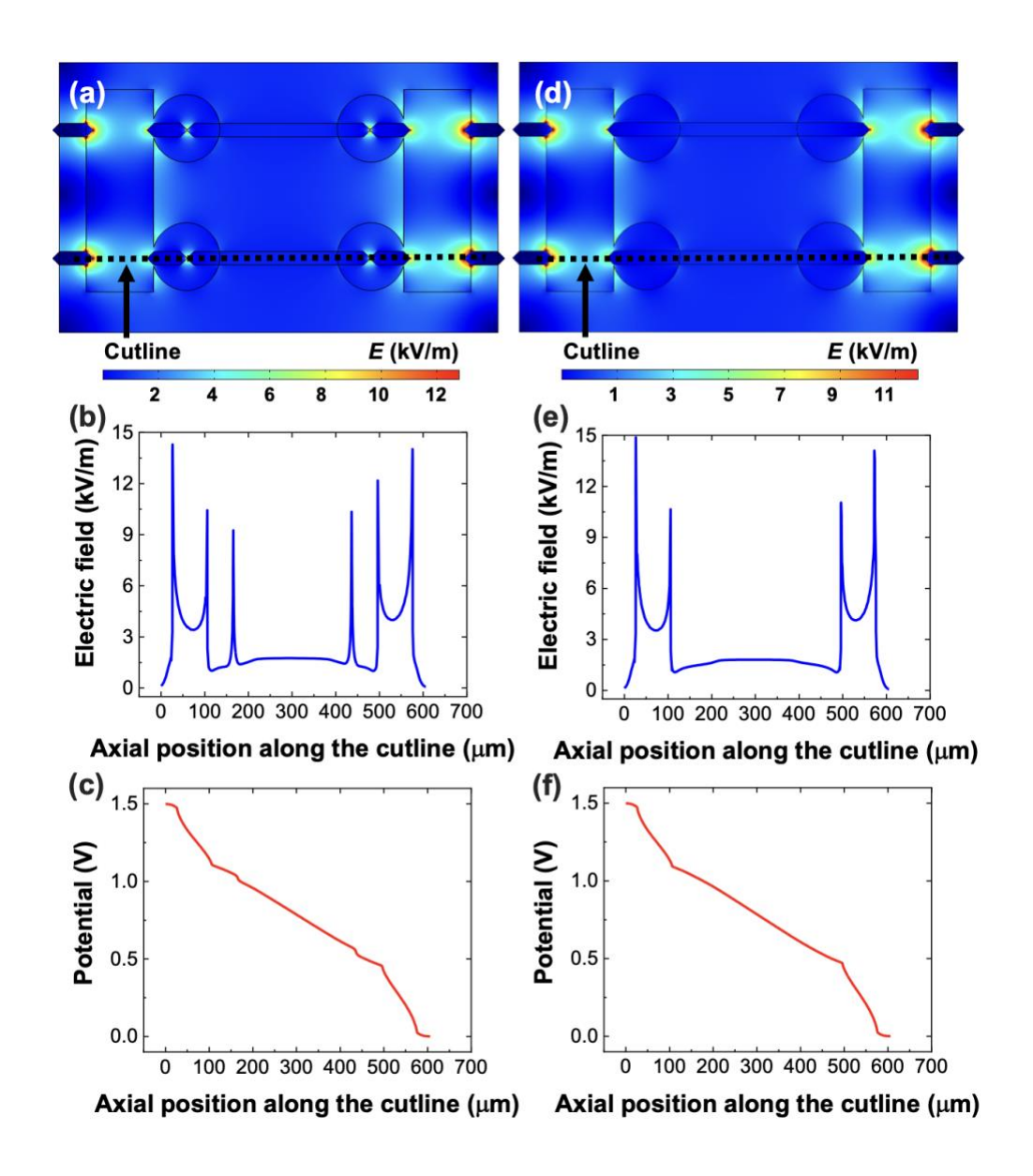


**Figure 1.** Numerical simulation showing the electric field distribution in an array of four fluidic chambers in the device designs with notched (a-c) and continuous (d-f) electrodes. (a,d) Surface plot of the electric field strength in the plane of the thin film electrodes. (b-f) Line plots of the electric field strength (b,e) and electric potential (c,f) along the cutline in (a,d).

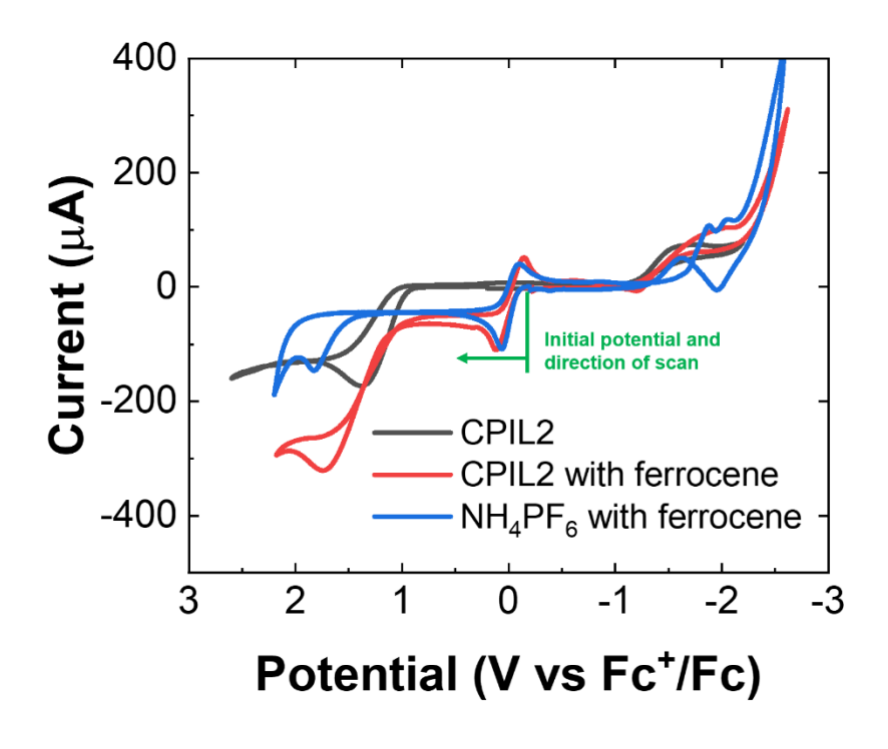


**Figure 2.** Cyclic voltammograms (CVs) of CPIL2 (10 μL/mL in CH<sub>3</sub>CN, with (red trace) and without (black trace) 6.0 mM ferrocene, which was included to provide a reference potential) obtained in a three-electrode cell. The background CV (blue trace) was completed in 6.0 mM ferrocene and 0.1 M NH<sub>4</sub>PF<sub>6</sub> (as supporting electrolyte) in CH<sub>3</sub>CN. A 3.0-mm diameter Pt disk electrode, a 0.5-mm diameter Pt wire and Pt mesh were used as working, reference, and auxiliary electrodes, respectively. Polymerization of CPIL2 occurs at 1.4 V vs. Fc/Fc+. Scan rate: 50 mV s<sup>-1</sup>.

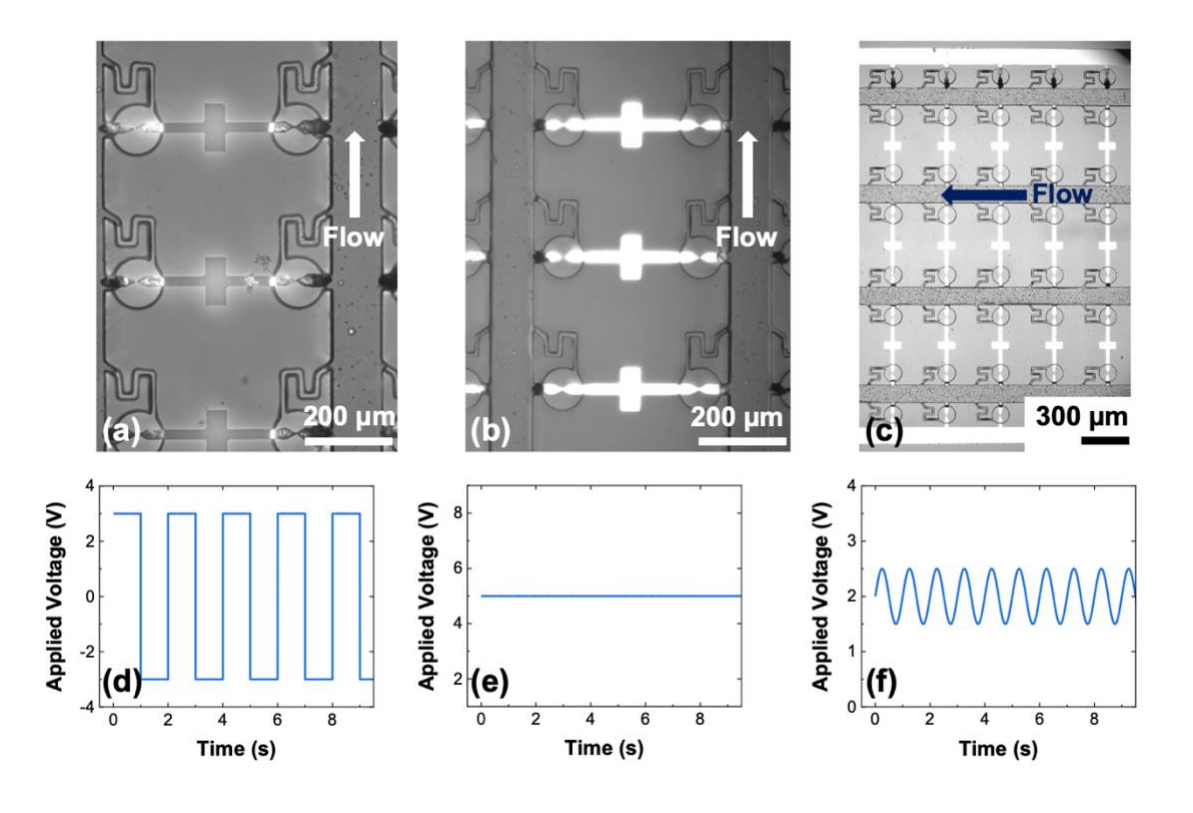


**Figure 3.** Deposition of neat CPIL2 in the multi-channel microfluidic device under three modes. Brightfield micrographs showing (a) symmetrical electropolymerization of CPIL under the electric waveform shown in (d), (b) dissymmetrical electrodeposition of CPIL under a DC voltage plotted in (e), and (c) regional electrodeposition of CPIL under the electric waveform shown in (f).

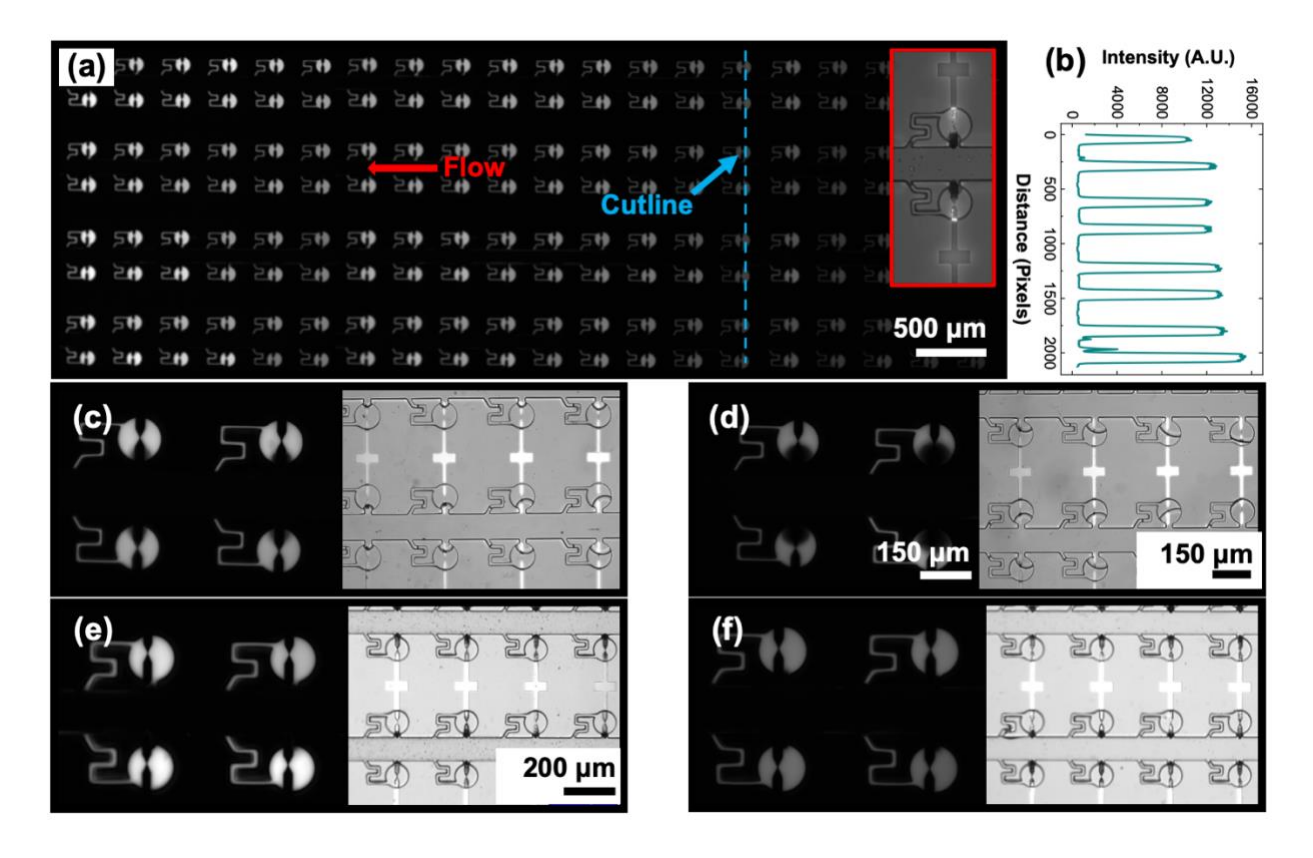
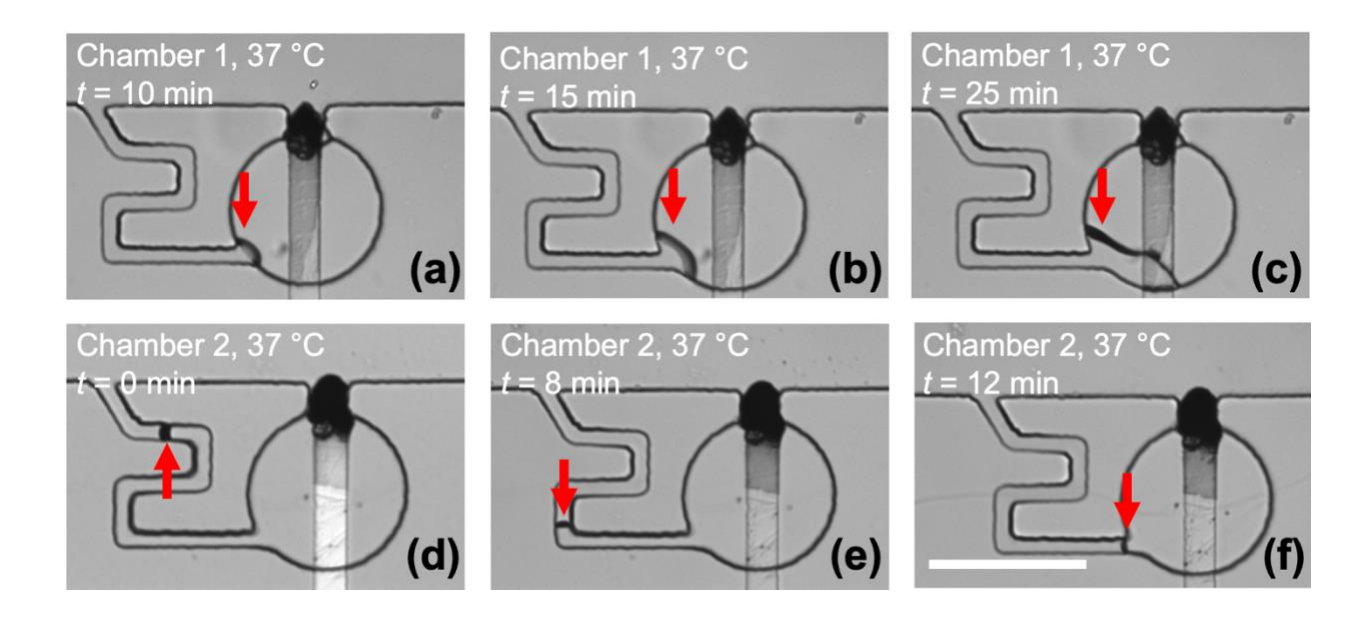


Figure 4. Isolation of the aqueous solution with the chambers with CPIL and CPIL polymer. (a) Fluorescence micrograph obtained immediately following electropolymerization under mode 1, t = 0 min. (b) Plot of the fluorescence intensity profile along the cutline in (a). In (c-f), paired fluorescence (left) and brightfield (right) micrographs show the phase boundary following isolation of the chambers with CPIL (c,d) and CPIL polymer (e,f) at t = 15 min (c,e) and t = 50 min (d,f).



**Figure 5.** Brightfield micrographs showing the robustness of the seal under conditions relevant to single-cell enzymatic assay. Images (a-f) are obtained for two chambers at three time points each. The CPIL-water boundary is progressing through the leak channel towards the chamber due to the negative pressure generated in the chambers by evaporation.

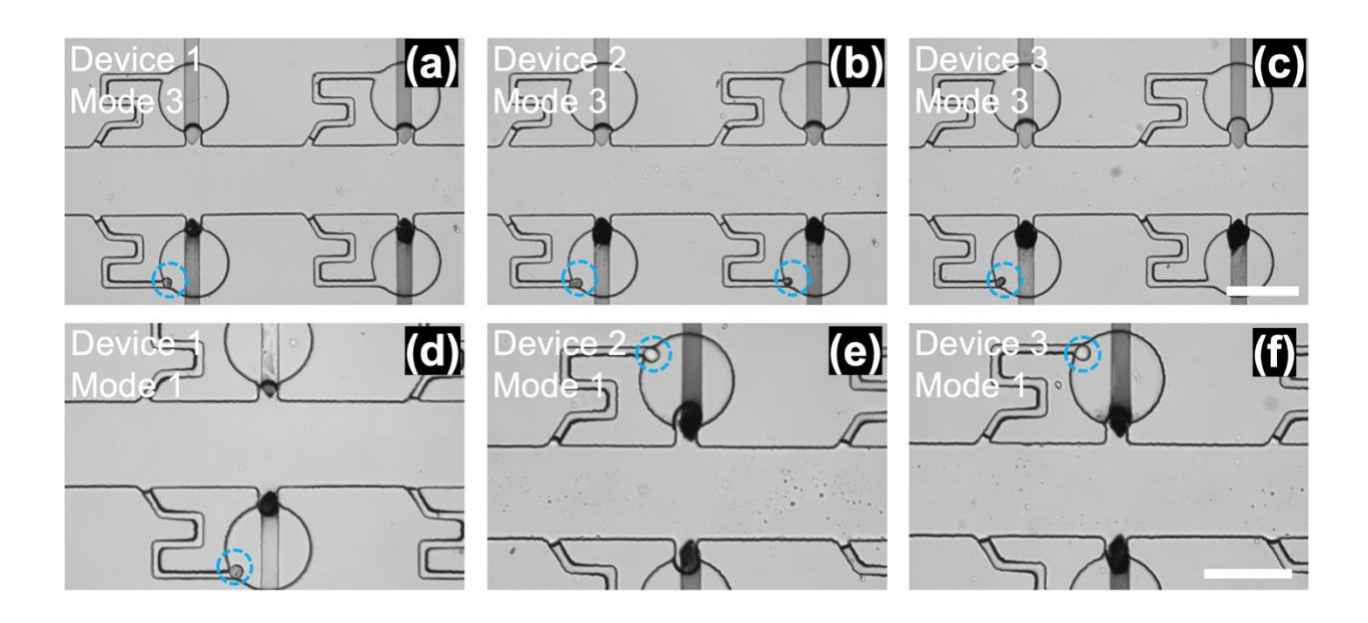


Figure 6. Brightfield micrographs showing isolation of single melanoma cells (SK-MEL-28) with CPIL polymer following their capture in individual chambers by DEP. Three replicates, carried out in separate devices, are shown for electropolymerization by each (a-c) mode 3 and (d-f) mode 1. Blue dashed circles indicate the position of a cell in each frame. Each cell is positioned within a chamber at the inlet to the 'leak' channel, which is utilized for hydrodynamic transfer of cells into the chambers. Scale bar is 100 μm.

# **Table of Contents Graphic**

